Twenty Years After: Hierarchical Core-Stateless Fair Queueing

Zhuolong Yu, Jingfeng Wu, and Vladimir Braverman, *Johns Hopkins University;* Ion Stoica, *UC Berkeley;* Xin Jin, *Peking University*

https://www.usenix.org/conference/nsdi21/presentation/yu

This paper is included in the Proceedings of the 18th USENIX Symposium on Networked Systems Design and Implementation.

April 12–14, 2021

978-1-939133-21-2

Twenty Years After: Hierarchical Core-Stateless Fair Queueing

Zhuolong Yu
Johns Hopkins University

Jingfeng Wu
Johns Hopkins University

Vladimir Braverman
Johns Hopkins University

Ion Stoica
UC Berkeley

Xin Jin
Peking University

Abstract

Core-Stateless Fair Queueing (CSFQ) is a scalable algorithm proposed more than two decades ago to achieve fair queueing without keeping per-flow state in the network. Unfortunately, CSFQ did not take off, in part because it required protocol changes (i.e., adding new fields to the packet header), and hardware support to process packets at line rate.

In this paper, we argue that two emerging trends are making CSFQ relevant again: (i) cloud computing which makes it feasible to change the protocol within the same datacenter or across datacenters owned by the same provider, and (ii) programmable switches which can implement sophisticated packet processing at line rate. To this end, we present the first realization of CSFQ using programmable switches. In addition, we generalize CSFQ to a multi-level hierarchy, which naturally captures the traffic in today's datacenters, e.g., tenants at the first level and flows of each tenant at the second level of the hierarchy. We call this scheduler Hierarchical Core-Stateless Fair Queueing (HCSFQ), and show that it is able to accurately approximate hierarchical fair queueing. HCSFQ is highly scalable: it uses just a single FIFO queue, does not perform per-packet scheduling, and only needs to maintain state for the interior nodes of the hierarchy. We present analytical results to prove the lower bounds of HCSFQ. Our testbed experiments and large-scale simulations show that CSFQ and HCSFQ can provide fair bandwidth allocation and ensure isolation.

1 Introduction

Fair queueing is a canonical mechanism to provide fair bandwidth allocation to network traffic by ensuring that each flow gets its fair share irrespective of the other flows. This way, fair queueing enforces isolation between competing flows, which ensures that normal flows are protected from ill-behaving flows. There is a long history of research on fair queueing [1–12]. Many of the proposed solutions require to maintain per-flow state in the switch, and rely on complex data structures and scheduling algorithms to realize fair queueing.

Core-Stateless Fair Queueing (CSFQ) [13] is a scalable algorithm to realize fair queueing. Compared to the alternatives, CSFQ has the unique property that it does not maintain per-flow state in the network. With CSFQ, the sources or switches at the edge classify traffic into flows and estimate per-flow rate. In turn, the switches in the network estimate the fair rate, and use probabilistic dropping to regulate each flow to its fair rate without maintaining per-flow state.

While CSFQ was proposed more than twenty years ago, it has not taken off. This is primarily due to two reasons. First, it requires changes to the IP protocol (i.e., adding a field to the IP header) and coordination across all switches (routers) in the network. Second, CSFQ requires switches to estimate the fair rate, compute a drop probability, and update the header of each packet. To perform these operations at line rate we need hardware support. These challenges are exacerbated by the fact that routers belong to different, often competing, Internet Service Provides (ISPs), which would all need to cooperate to upgrade their infrastructures to support CSFQ.

However, two emerging technologies are making CSFQ relevant again: (i) the advent of cloud computing and (ii) the increased popularity of programmable switches. Cloud providers own large datacenters consisting of many thousands of servers. Since a datacenter is typically owned by a single administrative entity (cloud provider) that controls both the software and hardware, it is relatively easy for a cloud provider to upgrade all its switches and servers to support CSFQ. FairCloud [14] proposes to apply CSFQ for network isolation in datacenters, but it does not have a hardware implementation for CSFQ. The emergence of programmable switches makes it possible to implement sophisticated packet processing at line rate. In particular, as we will show in this paper, existing programmable switches are powerful enough to support CSFQ at line rate.

While datacenter deployment removes the adoption barriers for CSFQ, it also raises new challenges. In particular, while CSFQ has been designed for a flat hierarchy, the traffic in today's datacenters is naturally structured in a multi-level hierarchy. For example, at the top level we typically have tenants and at the bottom level we have the flows of those tenants. The mechanism of choice to manage such traffic is hierarchical fair queueing [9,10,15], where each non-leaf node distributes its excess bandwidth (i.e., the bandwidths unused by some of its children) across its children. This allocation policy is consistent with a per-tenant payment granularity, i.e., network resources are divided between tenants in proportion to their payments [14]. In this case, if a flow of a tenant stops sending data, that tenant would want to re-allocate the flow's bandwidth to its other flows, and not to the flows of other tenants in the datacenter.

However, implementing hierarchical fair queueing is challenging. Existing solutions require per-flow state, and more importantly, require complex queue management and packet transfers in a hierarchy of queues [9, 10, 15]. Because of the implementation complexity, hierarchical fair queueing is not supported by today's high-speed hardware switches.

To address this challenge, we propose Hierarchical Core-Stateless Fair Queueing (HCSFQ). CSFQ only provides fair queueing, not hierarchical fair queueing. Directly extending CSFQ to support hierarchical fair queueing would require a hierarchy of queues. HCSFQ is able to accurately approximate hierarchical fair queueing and it is highly scalable. The key difference of our approach is that HCSFQ requires only a *single* queue, not a hierarchy of queues. HCSFQ also requires *no* packet scheduling. HCSFQ recursively computes the fair rate of each node starting from the root, and then limits the rate of each flow to its fair share rate. To the best of our knowledge, HCSFQ is the *first* solution that enables hierarchical fair queueing on commodity hardware at line rate while requiring neither per-flow state nor hierarchical queue management.

An important distinction of HCSFQ from CSFQ is that HCSFQ keeps the state of the interior nodes of the hierarchy in the switch. The state of the interior nodes is necessary to support hierarchical fair queueing, as the fair share rates of distinct interior nodes are typically *different*. The excess bandwidth of a flow is *only* shared with its *sibling* flows. That is, if a flow changes its sending rate, it would impact the fair rate of the sibling flows, but not necessarily of other flows in the hierarchy. Note that similar to CSFQ, HCSFQ does not maintain *per-flow* state (i.e., the state of the leaf nodes). Fortunately, for today's multi-tenant clouds, the number of tenants is orders of magnitude smaller than the number of flows, and commodity switches have sufficient on-chip memory to maintain the state for these interior nodes.

We exploit the capability of programmable switching to provide the first realization of CSFQ and HCSFQ on commodity hardware. While conceptually simple, implementing these schedulers on a programmable switch raises several technical challenges. First, they use a complex formula to estimate the rates, which includes several floating-point multiplication, divisions and exponentiation operations. Unfortunately, these operations are not supported by today's programmable switches. To get around this challenge, we leverage high-precision timestamps and a window-based mechanism to estimate these rates. Second, these algorithms rely on probabilistic packet dropping to limit the flows to their fair rates. Unfortunately, probabilistic packet dropping cannot be directly implemented in these switches. We discretize the probability computation to approximate the dropping probability with bounded error. To discretize these probabilities we leverage the switch's random number generator and take advantage of multiple stages. Third, computing the fair rate exhibits a circular dependency. Unfortunately, the switch data plane consists of a multi-stage processing pipeline, and the later stages cannot modify the state in the previous stages. To address it, we judiciously use packet recirculation, and periodically update the fair rate to minimize recirculation overhead.

In summary, we make the following contributions.

- We extend CSFQ to HCSFQ, the first scalable, practical solution to implement hierarchical fair queueing on commodity hardware at line rate with no per-flow state and no hierarchical queue management.
- We exploit the capability of programmable switching ASICs to provide the first data plane design for CSFQ and HCSFQ.
- We implement a prototype of CSFQ and HCSFQ on a Barefoot Tofino Wedge 100BF-65X switch. Our experiments show that CSFQ and HCSFQ can provide fair bandwidth allocation and ensure isolation.

2 Background and Motivation

Our work is motivated by the need for network isolation in multi-tenant datacenters. CSFQ is a scalable solution for fair queueing. We review the background of CSFQ, and identify the opportunities for CSFQ in modern datacenters.

2.1 Core-Stateless Fair Queueing

Fair queueing provides max-min fairness for competing flows. A max-min fair bandwidth allocation is one that any increase of the allocation to some flows would necessarily decrease the allocation of some other flows. The basic way to realize fair queueing in a switch is to keep one queue for each flow and use a scheduling algorithm to pick which queue to dequeue a packet each time. There has been decades of research on fair queueing [1–12]. While we leave the extensive discussion to related work (§7), we emphasize that most solutions are not scalable because of the need to maintain *per-flow* state to classify flows and shape their rates with per-flow queues and complex queue management. As a result, commodity switches only support 10–20 queues.

CSFQ is a *scalable* algorithm to achieve fair queueing with a unique property that it does *not* maintain per-flow state in the network. Figure 1 shows the architecture of CSFQ. CSFQ divides the network into edge and core. The switches

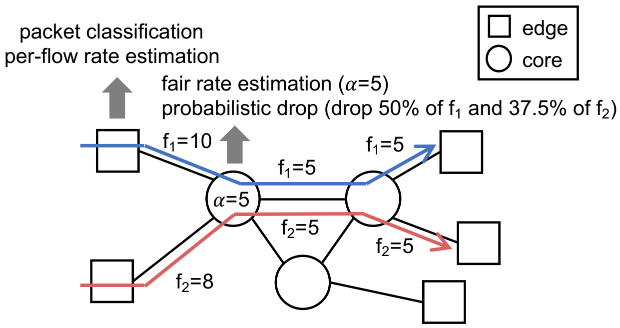

Figure 1: Core-Stateless Fair Queueing.

flow	f_1	f_2	f_3	f_4
arrival rate	1	4	5	5
bandwidth allocation	1	3	3	3

(a) Fair queueing.

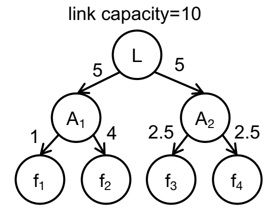

(b) Hierarchical fair queueing.

Figure 2: Fair queueing and hierarchical fair queueing.

or hosts at the edge, which do maintain per-flow state, use per-flow state to classify packets into flows and estimate per-flow arrival rate. Then the arrival rate of each flow is *carried* in a custom packet *header*. The switches in the core only estimate the *total* arrival rate of all flows, and then use it to estimate the *fair share rate* with an iterative algorithm. The switches compare the per-flow arrival rate in the packet header with the fair share rate to compute a drop probability, and drop packets to shape the rate of each flow to the fair share rate.

The key benefit of CSFQ is that the complexity (packet classification and flow rate estimation with per-flow state) is moved to the edge, making the core extremely simple. A core switch only maintains the state for *aggregate* variables (total arrival rate, total accepted rate and fair share rate), and only uses *one* queue for packet buffering. More importantly, the complexity of a core switch does *not* change with the number of flows, making the core scale-free.

2.2 Opportunities

CSFQ did not take off because it requires cooperation between ISPs to provide end-to-end isolation for Internet flows, and requires protocol and hardware changes. After twenty years, we believe the time for CSFQ has come because of two opportunities.

The first opportunity is from cloud computing. Cloud computing has become the fundamental infrastructure of today's Internet. Datacenters power large-scale Internet services we use everyday such as search, social networking and e-commerce, and enterprises are increasingly moving their workloads to the cloud. Fair bandwidth allocation and network isolation for datacenter networks is an important problem [14, 16–28]. While there has been many fair queueing algorithms proposed in the past [1–12], they are rarely deployed in practice because they need to maintain per-flow state in switches but switches can only support 10–20 queues. CSFQ provides a scalable solution to address this problem. Datacenter operators control the entire infrastructure, including both software and hardware. Adopting CSFQ to enforce isolation for datacenter networks naturally eliminates the need of cooperation between different operators or ISPs, as a datacenter network is under a single administrative domain.

The second opportunity is from programmable switching ASICs. Traditional switching ASICs are fixed-function, and adding a new feature like CSFQ requires switch vendors to design a new ASIC. Emerging programmable switching ASICs, such as Barefoot Tofino [29], Broadcom Trident 4 [30] and Cavium XPliant [31], allow users to program the data plane and develop new features. Specifically, to implement CSFQ on a programmable switch, we can program the parser to parse the custom header of CSFQ (to carry per-flow rate), program the match-action tables to implement the CSFQ algorithm, and program the on-chip memory to store the aggregate state. Because a datacenter network is under a single administrative domain, it is easy for the operator to adopt the protocol and hardware changes with programmable switching ASICs.

3 Hierarchical Fair Queueing

A multi-tenant cloud has a natural two-layer hierarchy, with the tenants at the first layer and the flows of each tenant at the second layer. Network isolation for multi-tenant datacenters naturally requires hierarchical fair queueing. CSFQ only supports fair queueing, but not hierarchical fair queueing. Hierarchical fair queueing provides fair queueing in a hierarchical manner. Flows are grouped into flow aggregates in multiple layers. The root of the tree includes all the flows. Each node in the tree includes a subset of the flows, called a *flow aggregate*, and fairly allocates its bandwidth to its child nodes. This is done recursively until leaf nodes, each of which contains one flow. The flows are broadly defined, e.g., based on five-tuple or network management considerations. In the case of multi-tenant clouds, it is a two-layer bandwidth allocation. The bandwidth is first allocated to the tenants in the first layer, and then each tenant allocates its bandwidth to its own flows in the second layer.

Fair queueing allocates bandwidth fairly to competing flows, and is work conserving, i.e., unused bandwidth share of a flow can be allocated to other flows. The key benefit of hierarchical fair queueing is that it allows unused share of a flow to be allocated to other flows in the same flow aggregate, instead of being shared by all the flows. Fair queueing can be considered as a special case of hierarchical fair queueing that contains only one layer. Two-layer fair queueing for multi-tenant clouds is desirable because the payment is based on

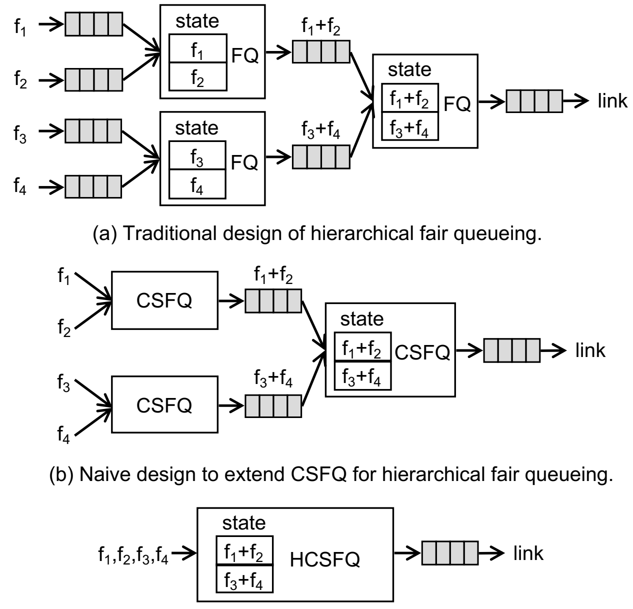

(a) Traditional design of hierarchical fair queueing.

(b) Naive design to extend CSFQ for hierarchical fair queueing.

(c) HCSFQ design.

Figure 3: Comparison of traditional hierarchical fair queueing design, naive design to extend CSFQ, and HCSFQ design.

per tenant. A tenant would want to share its bandwidth only between its own flows, as long as it has sufficient demand.

Example. We use an example in Figure 2 to contrast hierarchical fair queueing with fair queueing. There are four flows, i.e., f_1, f_2, f_3, and f_4. The arrival rates of the four flows are 1, 4, 5, and 5, respectively. The link capacity is 10. With only fair queueing, the unused share of f_1 is evenly allocated to all other three flows. As shown in Figure 2(a), the bandwidth allocation to the four flows is (1, 3, 3, 3). Suppose that f_1 and f_2 are in one flow aggregate (A_1), and f_3 and f_4 are in the other (A_2). With hierarchical fair queueing, the unused fair share of f_1 is only allocated to f_2, instead of also being shared by f_3 and f_4. Figure 2(b) shows the bandwidth allocation with two-layer hierarchical fair queueing, where the flows receive 1, 4, 2.5, and 2.5, respectively.

Challenge. Hierarchical fair queueing is known to be challenging to realize in switches at high speed. A traditional design to support hierarchical fair queueing is to leverage a hierarchy of queues, and each node in the hierarchy implements fair queueing for the queues of its child nodes. Figure 3(a) shows an example of such a design to support the two-layer hierarchy in Figure 2(b). This design has two major problems. First, the amount of state and the number of queues needed by this design is proportional to the number of nodes in the hierarchy. It needs to maintain per-flow state and the state of each interior node in the tree. Second, the design involves complex queue management with a hierarchy of queues, as packets need to be moved between queues in different layers. CSFQ does not require maintaining per-flow state, but naively extending CSFQ to support hierarchical fair queueing would still require a hierarchy of queues as shown in Figure 3(b). These two factors together make the design hard to scale to support a large number of flows. As a result, hierarchical fair queueing is not supported by today's high-speed switches.

4 HCSFQ Design

We propose Hierarchical Core-Stateless Fair Queueing (HCSFQ), which generalizes CSFQ to support hierarchical fair queueing. HCSFQ is the first scalable solution that enables hierarchical fair queueing on commodity hardware at line rate without per-flow state and complex hierarchical queue management.

We give a high-level overview of HCSFQ in Figure 3(c). In contrast to the traditional design in Figure 3(a), HCSFQ has two unique properties: (i) it does not maintain per-flow state, but only keeps the state of interior nodes; (ii) it does not require a hierarchy of queues, but only uses one queue. These two properties together dramatically simplify the design, making HCSFQ amenable to be implemented on high-speed switches under strict timing and resource constraints.

The major distinction between HCSFQ and CSFQ is that HCSFQ needs to maintain the state of interior nodes. This is necessary because HCSFQ aims to provide hierarchical fair bandwidth allocation for a flow hierarchy. Note that the naive design of extending CSFQ in Figure 3(b) also requires maintaining the state of interior nodes. In fair queueing, CSFQ only requires to keep one fair share rate, which is the same for *all* flows. But in hierarchical fair queueing, the fair share rates for different flows can be *different* if two flows are not siblings (i.e., do not have the same parent node). If a flow changes its rate, it would affect the fair share rate of its sibling flows, but not necessarily those of non-sibling flows. Figure 4 illustrates this with a concrete example. There is a two-layer hierarchy with four flows. At time T_1, the arrival rates for the four flows are 1, 4, 5, and 5 (the same as Figure 2). The fair share rate at L is 5, and those at A_1 and A_2 are 4 and 2.5. Then at time T_2, f_1 increases its arrival rate from 1 to 2. Then under fair bandwidth allocation, the new fair share rate for the subtree under A_1 becomes 3, so that f_1 receives 2 and f_2 receives 3. The rate change of f_1, however, does not effect the fair share rate for f_3 and f_4. This is because f_3 and f_4 are not sibling nodes of f_1.

CSFQ can be considered as a special case of HCSFQ which contains only one layer, and as such, it only carries the state for one interior node—the root.

4.1 Fluid Model

We first use a fluid model to formalize hierarchical fair queueing. The fluid model considers a switch with output link capacity C, and the flows are modeled as a continuous stream of bits. The flow hierarchy is represented as a directed graph $G(V,E)$, where V is the set of nodes and E is the set of edges.

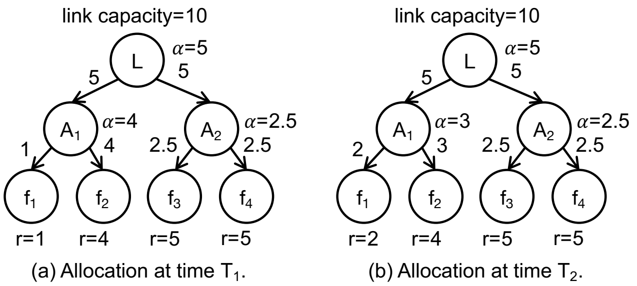

Figure 4: The flow arrival rates change from T_1 to T_2. It is necessary for the switch to keep the state for the interior nodes of the hierarchy in order to realize hierarchical fair queueing.

A node $v \in V$ represents a flow aggregate (i.e., a set of flows), where $r(v)$ is the arrival rate of the flow aggregate and $c(v)$ is the capacity allocated to v. A directed edge $e(v,u) \in E$ represents that u is a child of v.

Max-min fair bandwidth allocation ensures that the flows that are bottlenecked by a link receives the same output rate, which we call the fair share rate. Let $\alpha(v)$ be the fair share rate that node v allocates to its children. If max-min fair bandwidth allocation is achieved, for a child node u of node v, the flow aggregate at u receives a bandwidth allocation of $c(u) = min(r(u), \alpha(v))$. The arrival rate of v is the sum of the arrival rates of its children, i.e., $r(v) = \sum_{e(v,u)\in E} r(u)$. If $r(v) > c(v)$, the arrival rate of v exceeds the capacity allocated to v, and the fair rate $\alpha(v)$ is the unique solution to

$$c(v) = \sum_{e(v,u)\in E} \min(\alpha(v), r(u)). \tag{1}$$

If $r(v) \leq c(v)$, the arrival rate of v is no more than the capacity allocated to v, and all flows in v can be forwarded without dropping packets. In this case, by convention we have

$$\alpha(v) = \max_{e(v,u)\in E} r(u). \tag{2}$$

The fair rate computation is done recursively from the root to the leaf nodes. When v is the root, we have $c(v) = C$, where C is the link capacity. Then starting from the root, we can compute $c(v)$ and $\alpha(v)$ for each node in the tree.

Based on this fluid model, there is a simple algorithm to achieve max-min fair bandwidth allocation. In this algorithm, we first use the recursive computation to compute $\alpha(v.parent)$ for each leaf node v, which is the fair share rate allocated by v's parent to v. If $r(v) \leq \alpha(v.parent)$, then no bits need to be dropped; otherwise, a fraction of $(r(v) - \alpha(v.parent))/r(v)$ need to be dropped. Therefore, achieve max-min fair bandwidth allocation, each incoming bit of the flow in v is dropped by probability

$$\max(0, 1 - \frac{\alpha(v.parent)}{r(v)}). \tag{3}$$

4.2 HCSFQ Algorithm

The HCSFQ algorithm realizes the conceptual fluid algorithm in a real switch. Similar to CSFQ, HCSFQ does not maintain per-flow state, and only requires a single FIFO queue for packet buffering (Figure 3). The algorithm relies on two building blocks from CSFQ, which are arrival rate estimation and fair share rate estimation, and applies them recursively to compute the fair share rate for each leaf node.

Arrival rate estimation. The arrival rate estimation is used to estimate the arrival rate of a flow aggregate for a node in the hierarchy. Like CSFQ, it uses the canonical exponential averaging mechanism in networking for rate estimation. Let t_i and l_i be the arrival time and length of the i^{th} packet of the flow aggregate in node v. We use $r(v)$ to denote the estimated arrival rate of v. It is updated each time a new packet of v arrives, based on the following equation,

$$r(v)_{new} = (1 - e^{T_i/K})\frac{l_i}{T_i} + e^{T_i/K} r(v)_{old}, \tag{4}$$

where $T_i = t_i - t_{i-1}$ and K is a constant.

Fair share rate estimation. The fair share rate estimation is used to estimate the fair share rate that a node allocates to its children. The capacity of node v is $c(v)$. Eq.(4) gives the arrival rate of the node $r(v)$. If $r(v) \leq c(v)$, then $\alpha(v)$ is calculated using Eq.(2). Otherwise, $\alpha(v)$ should be the unique solution to Eq.(1). We apply the iterative algorithm in CSFQ to approximately solve the equation. Specifically, for each node v, we maintain the accepted rate estimation $f(v)$, which is updated with Eq.(4) if the packet is not dropped. Then, $\alpha(v)$ is approximately computed with the following formula,

$$\alpha(v)_{new} = \alpha(v)_{old} \frac{c(v)}{f(v)}. \tag{5}$$

Note that the computation of $\alpha(v)$ is iterative. It converges to the solution of Eq.(1) after several iterations, i.e., processing several packets. Similar to CSFQ, HCSFQ also uses a window of size K_c to account for inaccuracies introduced by exponential averaging in rate estimation. That is, $\alpha(v)$ is updated only if the node is congested ($r(v) > c(v)$) or uncongested ($r(v) \leq c(v)$) for an interval of length K_c.

Packet state. A packet *pkt* carries two pieces of state in the packet header, which are *pkt.r* and *pkt.nodes*.

- *pkt.r* is the arrival rate estimate of the flow the packet belongs to.
- *pkt.nodes* is a list of node IDs that indicate the flow aggregates the packet belongs to in the flow hierarchy, excluding the leaf. For example, in Figure 2, if a packet *pkt* belongs to f_1 or f_2, then $pkt.nodes = [L, A_1]$.

CSFQ only carries *pkt.r* in the packet header as there is no flow hierarchy. HCSFQ additionally carries *pkt.nodes* to track the set of flow aggregates the packet belongs to in the hierarchy. Similar to CSFQ, both *pkt.r* and *pkt.nodes* are

Algorithm 1 HCSFQ(pkt)

```
1:  cur_α ← 0
2:  for v ∈ pkt.nodes do
        // estimate arrival rate
3:      r[v] ← estimate_rate(pkt)
4:      cur_α ← α[v]
    // calculate drop probability
5:  prob ← max(0, 1 − cur_α/pkt.r)
6:  if prob > rand(0, 1) then
7:      drop_flag ← TRUE
8:  for v ∈ pkt.nodes do
        // estimate accepted rate
9:      if drop_flag is False then
10:         f[v] ← estimate_rate(pkt)
        // allocate bandwidth
11:     if v is root then
12:         c[v] ← link capacity
13:     else
14:         c[v] ← min(α[v.parent], r[v])
        // update fair share rate
15:     if r[v] > c[v] then
16:         if congest_flag[v] is FALSE then
17:             congest_flag[v] ← TRUE
18:             start_time ← current_time
19:         else if current_time − start_time > K_c then
20:             α[v] ← α[v] · c[v]/f[v]
21:             start_time ← current_time
22:     else
23:         if congest_flag[v] is TRUE then
24:             congest_flag[v] ← FALSE
25:             start_time ← current_time
26:             tmp_α[v] ← 0
27:         else if current_time − start_time ≤ K_c then
28:             child_r ← v.next = NULL ? pkt.r : r[v.next]
29:             tmp_α[v] ← max(tmp_α[v], child_r)
30:         else
31:             α[v] ← tmp_α[v]
32:             start_time ← current_time
33:             tmp_α[v] ← 0
34:     cur_α ← α[v]
    // drop or enqueue pkt
35: if drop_flag then
36:     drop(pkt)
37: else
38:     enqueue(pkt)
    // update the packet rate
39: pkt.r ← min(cur_α, pkt.r)
```

inserted at the edge. An edge switch (e.g., a software switch, a NIC or a ToR switch in datacenter networks) performs packet classification to get *pkt.nodes*, and uses Eq.(4) to estimate the flow rate *pkt.r*. Both *pkt.r* and *pkt.nodes* are transparent to end hosts and are removed by the switch at the last hop.

Hierarchical computation. The main difference between HCSFQ and CSFQ is that HCSFQ performs fair share rate estimation *recursively* in a hierarchical manner. In CSFQ, the arrival rate estimation for each flow is done at the edge, and a core switch only estimates the total arrival rate. In HCSFQ, because there is a hierarchy of flow aggregates, a core switch additionally estimates the arrival rate for each flow aggregate (i.e., the internal nodes in the tree). Similarly, in CSFQ, a

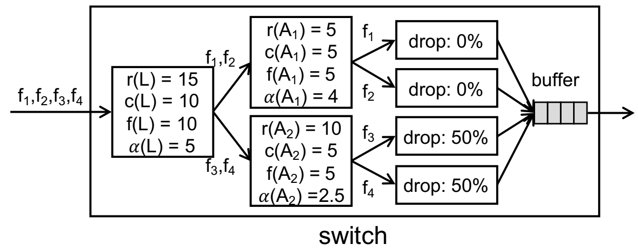

Figure 5: Example of the HCSFQ algorithm to provide hierarchical fair queueing for the scenario in Figure 2(b).

core switch only calculates a fair share rate for the link, while in HCSFQ, a core switch additionally calculates a fair share rate for each flow aggregate. Importantly, the fair share rate estimation in HCSFQ is used to *bridge* the computation of different layers together. That is, for node v, the allocated bandwidth $c(v)$ is used to estimate the fair share rate $\alpha(v)$, which is then used to compute the allocated bandwidth of its children, i.e., $c(u)$ for $u \in v.children$, in the next layer.

Algorithm 1 shows the pseudo code of the HCSFQ algorithm. When a packet *pkt* arrives at the switch, the switch updates the arrival rate estimate for each flow aggregate the packet belongs to using Eq.(4), and gets the fair share rate of the flow (line 1-4). Then the switch computes the dropping probability based on Eq.(3) and decides whether to drop the packet (line 5-7). After this, the switch recursively updates the fair share rate of each flow aggregate in the hierarchy (line 8-34). Based on whether the packet is dropped, the switch updates the accepted rate estimate for each flow aggregate (line 9-10). If node v is the root, then all flows are under this node, and its allocated capacity is the link capacity (line 11-12); otherwise, its allocated capacity is the max of the fair share rate allocated by its parent and its arrival rate (line 13-14). If the arrival rate of v is bigger than its allocated capacity, then the node is congested, and the fair share rate is updated based on Eq.(5) (15-21); otherwise, the fair share rate is the max arrival rate of its children, i.e., based on Eq.(2) (line 22-33). Note that we use a window of length K_c for fair share update to account for inaccuracies in rate estimation. Based on the dropping decision, the switch drops or enqueues the packet (line 35-38). Finally, the arrival rate *pkt.r* is updated and will be used by the next-hop switch (line 39). Note that the loops (line 2-4 and line 8-34) are done in one pass and the fair share rate is updated based on $c[v.parent]$ from the last round.

Figure 5 illustrates how the algorithm works to realize hierarchical fair queueing for the example in Figure 2. At the root, the total arrival rate of all flows $r(L)$ is 15, and the capacity $c(L)$ is the link capacity 10, which is below the arrival rate. The root fairly allocates the capacity to the two flow aggregates, A_1 and A_2. The figure shows the stable state when the accepted rates and fair share rates of all the nodes have converged. After convergence, the accepted rate $f(L)$ is 10, and the fair share rate $\alpha(L)$ is 5. At node A_1, the arrival rate $r(A_1)$, which is the sum of $r(f_1)$ and $r(f_2)$, is 5, and the allocated capacity $c(A_1)$ is 5. The fair share rate is set as 4, and there is no need to drop packets for f_1 and f_2. At node A_2, the arrival rate $r(A_2)$, which is 10, is bigger than the allocated capacity, which is 5. A_2 allocates its capacity to f_3 and f_4 fairly. Each receives a fair share rate of 2.5. So the switch drops 50% of the packets for both f_3 and f_4.

Weighted HCSFQ. The HCSFQ algorithm can be extended to support flows and flow aggregates with weights. For node v, we use $w(v)$ to represent the weight of the flow or flow aggregate of v. Under max-min fair bandwidth allocation, competing flows or flow aggregates at the bottlenecked link have the same fair share rate $r(v)/w(v)$. There are two changes to the algorithm in order to incorporate the weight. The first change is on the equation to compute the fair rate $\alpha(v)$ when $r(v) > c(v)$. Eq.(1) is changed to

$$c(v) = \sum_{e(v,u)\in E} w(u) \cdot min(\alpha(v), \frac{r(u)}{w(u)}). \tag{6}$$

The second change is on the equation to compute the drop probability. Eq.(3) is changed to

$$\max(0, 1-\alpha(v.parent) \cdot \frac{w(v)}{r(v)}). \tag{7}$$

4.3 Theoretical Guarantee

We have the following theorem to provide the theoretical guarantees for HCSFQ. The proof of the theorem is in Appendix.

Theorem 1. *Consider a link with a hierarchical fair queueing policy and a flow in the hierarchy. Let w_1, w_2, ..., w_n be the weights of the nodes from the root to the flow. Let α_1, α_2, ..., α_n be the constant normalized fair rate of the nodes from the root to the flow. Let $r_{\alpha_i} = \alpha_i w_i$. If probabilistic dropping is applied at the last layer, then the excess service received by the flow that sends at a rate at no larger than R, is bounded above by*

$$r_{\alpha_n} K(1+ln\frac{R}{r_{\alpha_n}}) + l_{max} \tag{8}$$

where l_{max} is the maximum packet length.

Consider a parent and its children in the hierarchy. Let the number of children be k. Let $r_{\alpha'}$ be the weighted fair rate of the parent, and $r_\alpha^{(j)}$ be the weighted fair rate of the j-th child. Suppose the inter-arrival time of every packet is at least τ, and

$$r_{\alpha'} \geq \frac{1}{1-e^{-\tau/K}} \sum_{j=1}^{k} r_\alpha^{(j)}.$$

The the parent node does not drop packets.

Remark. The first conclusion bounds the excess service that can be received by a flow. The second conclusion provides the theoretical condition for only performing probabilistic dropping at the leaf node.

5 Data Plane Design and Implementation

In this section, we describe a data plane design to implement CSFQ and HCSFQ on new-generation programmable switches. Programmable switches enable users to program the multi-stage match-action pipeline in the switch data plane to implement custom features. Users can also access the on-chip memory and implement stateful operations using the register arrays provided by programmable switches. Programmable switches also support a set of primitive actions (e.g., recirculate, bit shift, add and subtract) which make HCSFQ possible. Based on the constructs of programmable switches, we show how to design and implement the rate estimation, the fair rate computation and the flow shaping logic (i.e., Algorithm 1) on programmable switches. Our HCSFQ implementation contains 1952 lines of code in P4 and is compiled to Barefoot Tofino ASIC [29]. The code is open-source and available at https://github.com/netx-repo/HCSFQ.

5.1 Single Layer

We first describe how to implement CSFQ, i.e., single-layer HCSFQ, which is used as a building block to implement multi-layer HCSFQ. There are three challenges to implement single-layer HCSFQ on programmable switches: rate estimation, probabilistic drop, and fair rate update. We describe each challenge and its solution as follows.

Rate estimation. The switch needs to estimate two rates: the total arrival rate r, and the accepted rate f. Both rates are estimated with Eq.(4). Because switches have strict timing and resource requirements, an action in a match-action table can only contain a small number of operations in a limited operation set. The equation cannot be directly implemented in the switch data plane due to two reasons. First, the equation involves several multiplication, division and exponentiation operations on floating points. These operations are quite complex and require multiple clock cycles to compute. As such, they are not typically supported by the switch data plane. Second, a rate (r or f) is stored in a register of the on-chip memory. To update the rate, the switch needs to read the rate from the register, uses the equation to calculate the new rate, and then updates the register. A register can only be accessed by its own stage, but the equation includes multiple arithmetic operations, which requires multiple stages to compute.

We leverage the high-precision timestamps available in the data plane, and use a window-based mechanism to estimate the rates. Programmable switches are able to provide high-precision timestamps at the granularity of one nanosecond. To estimate a rate, the switch maintains a pair of registers (*reg.byte* and *reg.start*). One register (*reg.byte*) stores the total bytes of packets the switch has received in the current window. The other register (*reg.start*) stores the start timestamp of the current window. For each incoming packet, the switch first checks the current timestamp and compares it with $reg.start$ to see if the packet belongs to the current window. If so, the switch adds the size of the packet to $reg.byte$; otherwise, the switch clears $reg.byte$ and sets $reg.start$ to the current timestamp. The switch keeps another register $reg.rate$ to store the current rate estimate. When a window is passed, the switch uses $reg.byte$ to update $reg.rate$, which can be done with either a direct assignment, or a moving average. Our experiments indicate that using a moving average (implemented with several bit shift and addition operations) works better and avoids oscillation with the control loop that updates the fair share rate and drops packets.

The key benefit of this window-based mechanism is that because the switch can provide nanosecond-granularity timestamps, we can use a small window size to accurately estimate flow rate and capture sudden packet bursts. It is important to note that the rate estimation is local to the switch and only uses timestamps to divide time into windows. So there is no need for time synchronization between switches.

Probabilistic drop. Probabilistic drop is used to regulate the flows to the fair share rate. The switch uses the fair share rate α and the flow arrival rate r to compute the probability to drop packets of the flow (Eq.(3) and line 5 in Algorithm 1). Then the switch checks the condition $max(0, 1-\alpha/r) > rand(0,1)$ to decide whether to drop an incoming packet or not. Similar to rate estimation, the challenge is that switches do not support the division operation to compute the probability. One way to solve the problem is to use a similar window-based mechanism as rate estimation, i.e., divide time into windows with window size δ, and keep counters to allow up to $r\delta$ packets to pass in each window and drop all remaining packets. The drawback of this approach is that it introduces bursty packet drops, which do not work well with congestion control. We want to mimic the behavior of CSFQ to have random packet drops that are uniformly distributed in the packet stream.

We discretize the probability computation to approximate the drop probability with bounded error. We leverage the random number generator provided by the data plane and use multiple stages to realize the discretized computation. Specifically, to check the condition $max(0, 1-\alpha/r) > rand(0,1)$, it is sufficient to check $rand(0,1) > \alpha/r$. We multiply r to both sides of the inequality, and transform the condition to

$$rand(0,r) > \alpha.$$

If the switch can generate a random number between 0 and r, then we can simply compare the generated random number and α to decide whether to drop a packet. However, some switches can only generate a random number in a range of a power of two, i.e., in $[0, 2^n-1]$, where n is a given value at compilation time and cannot be a variable. One possible solution is to use a large value for n at compilation time and use $rand(0, 2^n-1)\%r$ to approximate $rand(0,r)$. But the modulo operation on an arbitrary number may not be supported, and the generated numbers are not uniformly distributed in $[0,r]$. We solve this problem by discretizing the probability computation. We use an integer, instead of a floating point, for the probability. We convert the condition to

$$rand(0, 2^n-1) \cdot r > (2^n-1) \cdot \alpha.$$

While multiplication is not directly supported, we can convert a multiplication operation into several bit shift and addition operations. Since n is small and one stage can do multiple operations, a multiplication can be done in a few stages. This solution introduces errors because the random number is an integer in $[0, 2^n-1]$, instead of a real number in $[0,1]$. However, the error is bounded by $1/2^n$, which reduces exponentially with n. When n is 7, the error introduced by the approximation is bounded by 1/128, which is smaller than 1%.

Fair rate update. When the link is congested, the fair share rate is the unique solution to Eq.(1). Because HCSFQ does not maintain per-flow state, it uses $\alpha_{new} = \alpha_{old} c/f$ (Eq.(5)) to approximately compute the fair share rate, where c is the capacity and f is the accepted rate. Like rate estimation and probabilistic drop, Eq.(5) cannot be supported because it contains multiplication and division. What is more challenging is that the fair rate update introduces the following circular dependency to the packet processing.

$$\text{read } \alpha \rightarrow \text{enqueue/drop} \rightarrow \text{update } f \rightarrow \text{update } \alpha$$

Specifically, the switch needs to read α to compute the drop probability. Then based on whether to enqueue or drop a packet, the switch updates the accepted rate f, which is then used to update α. Because a register can only be accessed by its own stage, the new value of α cannot be used to update the register that stores α in a previous stage.

To address these two problems, we first observe that the update equation $\alpha_{new} = \alpha_{old} c/f$ in HCSFQ is already an approximation, and the correct α is iteratively computed after several updates until f converges to c. As such, we replace the update equation with an additive-increase multiplicative-decrease method, which increases or decreases α each time if f is not equal to c. This ensures that the value for α converges to the correct value. Note that in the original CSFQ, α is also computed iteratively to converge to the correct value.

To address the circular dependency, we leverage packet recirculation available in programmable switches, and let the recirculated packets carry the new value of α to update the register for α in a previous stage. Switches have limited bandwidth for recirculation. We judiciously use packet recirculation to minimize recirculation overhead. We follow the same scheme as CSFQ: update α only when the node is congested or uncongested for a window length of K_c. Given the window size K_c, α is updated by at most $1/K_c$ times per second. As a concrete example, let K_c be 10 μs. Then α is updated by at most 100K times per second, and the amount of recirculation traffic is only a tiny fraction of the switch capacity.

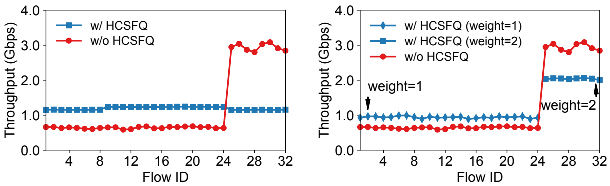

(a) Equal weights. (b) Different weights.

Figure 6: Testbed experiments of fair queueing for UDP. Flow 1–24 send at 2Gbps and Flow 25-32 send at 8Gbps.

5.2 Multiple Layers

The single-layer design is used as a building block to support multiple layers. As shown in Algorithm 1 and Figure 5, the processing of HCSFQ on a packet is performed layer by layer, from the root to the leaf node. This well matches the multi-stage packet processing pipeline of programmable switches. The layers in HCSFQ can be mapped to the stages in the pipeline, which naturally processes packets sequentially stage by stage. The major difference between HCSFQ and CSFQ is that HCSFQ needs to store more states as it has multiple layers. CSFQ is a single-layer HCSFQ and only maintains the state for three variables, which are the total arrival rate r, the accepted rate f, and the fair share rate α. Each variable use multiple registers as described in §5.1. HCSFQ maintains the state for all interior nodes, each of which includes the three variables. Commodity switches have 10-100 MB on-chip memory [32], which is able to support a large number of interior nodes. For a two-layer HCSFQ for tenant-level and flow-level isolation in multi-tenant datacenters, a switch needs to maintain per-tenant state, but not per-flow state. With 10-100 MB memory, the switch can support millions of tenants. In terms of the number of layers, our prototype supports up to four layers on Barefoot Tofino. There is no theoretical limit on the number of layers given the scalable algorithm design. The constraints for practical implementations mainly come from the restricted hardware primitives to implement the algorithm as we describe in §5.1. These constraints are not fundamental. Newer programmable switches (e.g., Barefoot Tofino 2) have more stages and provide more hardware primitives to support more layers. Despite this, we expect HCSFQ with 2–4 layers should be sufficient to provide hierarchical isolation for many datacenter scenarios (e.g., multi-tenancy).

6 Evaluation

In this section, we provide experimental results to demonstrate the performance of HCSFQ. We first evaluate the performance of single-layer HCSFQ (i.e., CSFQ), and show that it can provide fair queueing (§6.1). We then evaluate the performance of two-layer HCSFQ, and show that it can provide hierarchical fair queueing to enforce tenant-level and flow-level isolation for multi-tenant datacenters (§6.2). Finally, we use simulations to evaluate HCSFQ in a large-scale datacenter environment and compare it with several alternatives (§6.3).

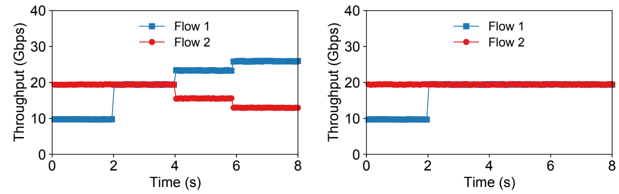

(a) w/o HCSFQ. (b) w/ HCSFQ.

Figure 7: Testbed experiments of fair queueing for UDP. Flow 1 is sending at a different rate every 2 seconds. Flow 2 is sending at 20Gbps.

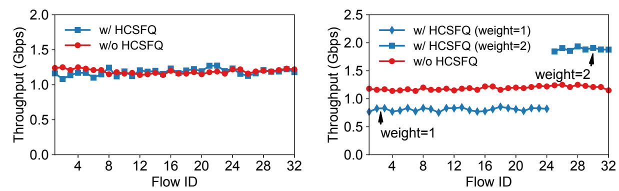

(a) Equal weights. (b) Different weights.

Figure 8: Testbed experiments of fair queueing for TCP.

All testbed experiments are conducted on a hardware testbed with a Barefoot Tofino Wedge 100BF-65X switch. Each server is configured with an 8-core CPU (Intel Xeon E5-2620 @ 2.1GHz), 64GB memory and one 40G NIC (Intel XL710), and runs Ubuntu 16.04.6 LTS with Linux kernel 4.10.0-28-generic. Our switch implementation contains both the edge and core functionalities for HCSFQ. Therefore, our prototype provides hierarchical fair queueing *without* modifications to either the software or hardware of the end hosts. By default, we use TCP Cubic provided by the Linux kernel.

6.1 Fair Queueing Experiments

We first evaluate the capability of HCSFQ to provide fair queueing. Fair queueing requires one-layer HCSFQ. We cover both UDP and TCP traffic with equal or different weights. In the experiments, we use four servers as the senders and one server as the receiver. Each sender sends 8 flows (based on five-tuple), and a total of 32 flows are sent to a receiver. All servers are connected to the switch with 40Gbps links. The bottleneck link is the link between the switch and the receiver.

UDP. If all UDP flows have the same sending rate, they would get similar bandwidth under the tail-drop FIFO queue in the switch. To make the experiment more interesting, we assign different sending rates to the UDP flows. We let 24 flows (Flow 1–24) send at 2Gbps and 8 flows (Flow 25–32) send at 8Gbps. As shown in Figure 6(a), without HCSFQ, Flow 25–32 obtain higher bandwidth than Flow 1–24 because Flow 25–32 have larger sending rates. In comparison, HCSFQ is able to fairly allocate bandwidth to the flows.

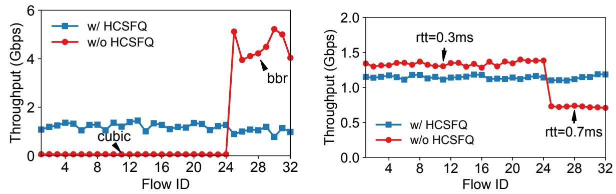

(a) Different TCP algorithms. (b) Different RTTs.

Figure 9: Testbed experiments of fair queueing for TCP under different configurations.

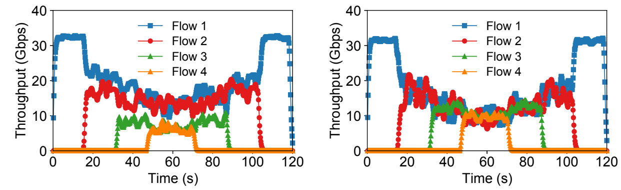

(a) Without HCSFQ. (b) With HCSFQ.

Figure 11: Testbed experiments of TCP convergence. Flow 1 and 2 have 0.3ms RTT, and Flow 3 and 4 have 0.7ms RTT.

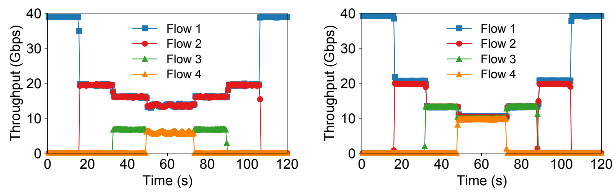

(a) Without HCSFQ. (b) With HCSFQ.

Figure 10: Testbed experiments of UDP convergence. Flow 1 and 2 send at 40Gbps, and Flow 3 and 4 send at 20Gbps.

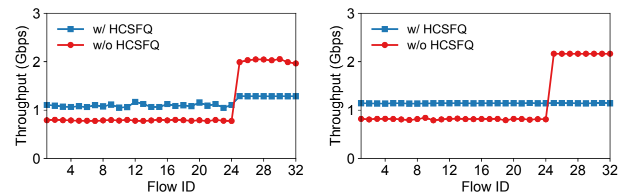

(a) Testbed experiment. (b) Packet-level simulation.

Figure 12: Evaluation result of mixed TCP and UDP traffic.

HCSFQ supports weighted fair queueing. We assign weight 1 to Flow 1–24 to and weight 2 to Flow 25–32. As shown in Figure 6(b), without HCSFQ, the result is the same as that with equal weights in Figure 6(a). On the other hand, HCSFQ is able to allocate the bandwidth based on the weights. Flow 25–32 achieve higher throughput than Flow 1–24.

We also evaluate HCSFQ when the UDP flows dynamically change their rates. We let Flow 1 send at a different rate every 2 seconds (10Gbps, 20Gbps, 30Gbps and 40Gbps, respectively) and let Flow 2 keep sending at 20Gbps. Without HCSFQ, when the link is congested (from 4s to 8s), each flow achieves a throughput in proportional to its sending rate. With HCSFQ, two flows get the fair share (20Gbps) when the link is congested.

TCP. Figure 8(a) shows the throughput of the flows with and without HCSFQ. Because TCP congestion control provides fair bandwidth allocation, the flows have similar throughput even without HCSFQ. Adding HCSFQ to the switch does not change the bandwidth allocation and thus has a similar result.

However, TCP cannot support weighted fair queueing. To show the benefits of HCSFQ, we let Flow 1–24 have weight 1 and Flow 25–32 have weight 2. Without HCSFQ, the result in Figure 8(b) is similar to that in Figure 8(a). With HCSFQ, the flows get bandwidth in proportional to their weights. The flows with higher weights (Flow 25–32) receive more bandwidth than those with lower weights (Flow 1–24).

Different TCP algorithms. There are many TCP congestion control algorithms. Without in-network enforcement, the flows using aggressive congestion control algorithms would get more bandwidth. In this experiment, we let Flow 1–24 use TCP Cubic (provided by default in Linux) and Flow 25–32 use TCP BBR. As shown in Figure 9(a), without HCSFQ, because TCP BBR is more aggressive than TCP Cubic, the flows with TCP BBR get almost all the bandwidth. On the other hand, HCSFQ is able to provide fair queueing, regardless of the TCP algorithms they use. We have also tried TCP Reno, which performs similar to TCP Cubic.

Different RTTs. In this experiment, we increase the RTT of Flow 25–32 by 0.4 ms using Linux Traffic Control (Linux tc). The default RTT measured by ping in the testbed, i.e., the RTT of Flow 1–24, is 0.3 ms (mostly host overhead). The TCP throughput is inverse proportional to RTT [33]. In our case, the flows with 0.3 ms RTT (Flow 1–24) should have $0.7/0.3 \approx 2\times$ higher bandwidth than the flows with 0.7 ms RTT (Flow 25–32), which is close to what we see in Figure 9(b). On the other hand, HCSFQ is able to provide fair queueing even when the flows have different RTTs.

Convergence. We let four flows from different clients join and leave a link every 16 seconds to evaluate convergence. Figure 10 shows the UDP result. Flow 1 and 2 send at 40Gbps (using DPDK [34]), and Flow 3 and 4 send 20Gbps. When HCSFQ is enabled, the four flows quickly converge to a similar rate, even though they have different sending rate. Figure 11 shows the TCP result. We set the RTTs of Flow 3 and 4 to 0.7ms using Linux tc, and the RTTs of of Flow 1 and 2 are around 0.3ms by default. With HCSFQ, the four flows quickly converge to a similar rate, regardless of different RTTs.

Mixed UDP and TCP traffic. We evaluate HCSFQ under a mixed workload with both UDP and TCP traffic, and consider the impact of ill-behaved UDP flows on TCP flows. In the experiment, Flow 1–24 are TCP flows, and Flow 25–32 are UDP flows that send at 3.2Gbps. As shown in Figure 12(a), without HCSFQ, because UDP flows are not affected by TCP

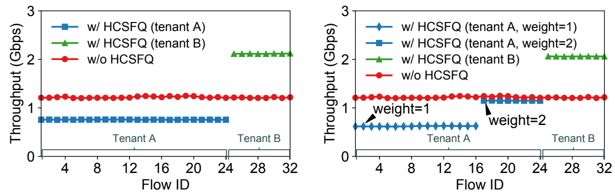

(a) Equal weights. (b) Different weights.

Figure 13: Testbed experiments of hierarchical fair queueing for UDP. Two tenants should have the same *total* throughput.

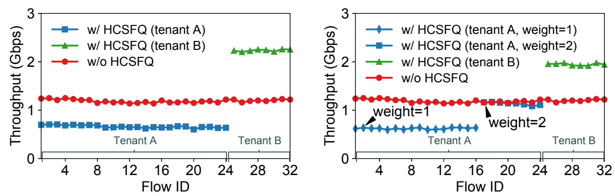

(a) Equal weights. (b) Different weights.

Figure 14: Testbed experiments of hierarchical fair queueing for TCP. Two tenants should have the same *total* throughput.

congestion control, Flow 25–32 get 84% higher throughput than their fair share. In comparison, HCSFQ is able to allocate bandwidth fairly between all flows.

Gap between prototype implementation and theoretical algorithm. Although the above experiment demonstrates the effectiveness of HCSFQ on protecting TCP flows from aggressive UDP flows, there is still a small gap from the theoretical upper bound. Figure 12(b) shows the simulation result on the same setup using a packet-level simulator Netbench [35]. In the simulation, the TCP and UDP flows get almost identical throughput with HCSFQ. The reason for the gap between Figure 12(a) and Figure 12(b) is that to realize HCSFQ on a real switch, we make several approximations described in §5. These approximations cause extra jitters for TCP flows, and UDP flows occupy the spare bandwidth caused by the jitters and obtain higher throughput. We believe as programmable switches get more capable, these approximations can be removed to enable more accurate implementation of HCSFQ in the future.

6.2 Hierarchical Fair Queueing Experiments

We now evaluate the capability of HCSFQ to provide hierarchical fair queueing. We show that two-layer HCSFQ can provide tenant-level and flow-level isolation for multi-tenant datacenters. Similar to the previous experiments, we use 4 servers to send a total of 32 flows to a receiver. To evaluate hierarchical fair queueing, we let tenant A contain 24 flows (Flow 1–24) and tenant B contain 8 flows (Flow 25-32).

UDP. We set the sending rates of all 32 UDP flows to 8 Gbps. As shown in Figure 13(a), without HCSFQ, the flows have

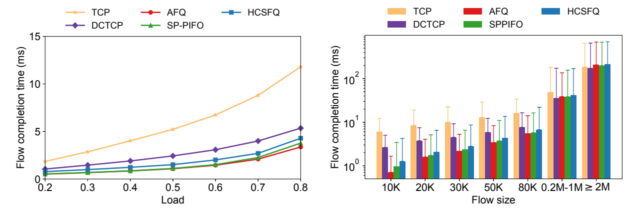

(a) Average flow completion time for flows less than 100KB. (b) Flow completion time (avg. and 99th) breakdown for 70% load.

Figure 15: Simulation result under the web search workload.

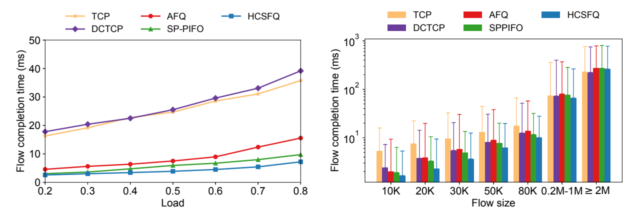

(a) Average flow completion time for flows less than 100KB. (b) Flow completion time (avg. and 99th) breakdown for 70% load.

Figure 16: Simulation result under the web search workload with injected UDP traffic.

similar throughput. Because tenant A has three times as many flows as tenant B, the total throughput of A is three times as that of B. With HCSFQ, two tenants get the same total throughput. Because A has more flows, each flow in A has lower throughput than that in B.

To evaluate weighted hierarchical fair queueing, we assign different weights to tenant A's flows. We let Flow 1–8 have weight 2 and Flow 9–24 have weight 1. We assign the same weight to tenant A and B. As shown in Figure 13(b), the result without HCSFQ is the same as it in Figure 13(a). All flows receive the same bandwidth, regardless of tenants and weights. With HCSFQ, because the two tenants have the same weight, the bandwidth allocation to the two tenants stays the same. In tenant A, a flow with weight 2 has double throughput as a flow with weight 1. In tenant B, all flows have the same weight, and thus they have the same throughput.

TCP. TCP congestion control does not recognize tenants. Figure 14(a) shows the throughput of 32 TCP flows. Similar to the UDP experiment, without HCSFQ, every flow receives the same amount of bandwidth, and tenant A has higher total throughput. With HCSFQ, the bandwidth is allocated equally to the two tenants, and each flow in A has lower throughput than each flow in B. We also assign weights to the TCP flows as the UDP experiment, and the result is in Figure 14(b). Similarly, with HCSFQ, Flow 1–8 in tenant A have lower throughput than Flow 9–24, because Flow 1–8 lower higher weight. The flows in tenant B have the same throughput because we do not change their weights.

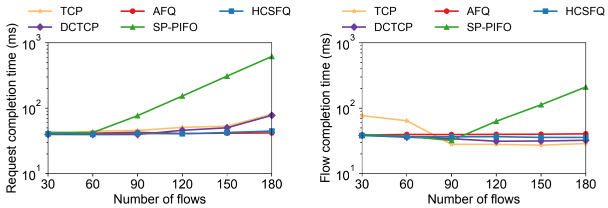

(a) Total request.

(b) Individual flows.

Figure 17: Simulation result under the incast scenario.

6.3 Large-Scale Simulation

We use simulations to evaluate HCSFQ in a large-scale datacenter environment. The simulations are conducted with a packet-level simulator Netbench [35]. Following the setting in SP-PIFO [12], we use a leaf-spine topology with 144 servers, 9 leaf switches and 4 spine switches, and set the access and leaf-spine links to 1Gbps and 4Gbps, respectively. We compare HCSFQ with TCP, DCTCP, and two state-of-the-art approaches AFQ (32 queues) [11] and SP-PIFO (32 queues) [12]. As in [11, 12], we enable ECN marking and use DCTCP as the transport layer for HCSFQ, AFQ and SP-PIFO.

Web search workload. We generate traffic based on the web search workload [36]. Figure 15(a) shows the flow completion time (FCT) for small flows less than 100KB, and Figure 15(b) shows the flow completion time breakdown when the network is at 70% utilization. HCSFQ achieves up to 60% lower FCT than vanilla TCP and DCTCP. AFQ and SP-PIFO are 15% better than HCSFQ on FCT because HCSFQ enforces fairness by packet dropping and cannot provide guarantee for sensitive packets which can be a drawback for datacenter workload. However, the gap is small and does not grow as the traffic load gets larger. The result demonstrates that HCSFQ is compatible with DCTCP, and can provide significant improvement under a representative datacenter topology and workload as the smaller flows can finish faster with a fair share rate.

Web search workload with injected UDP traffic. To evaluate performance isolation, we inject additional ill-behaved UDP flows to the web server workload. The UDP flows are evenly distributed in the topology and occupy about half of the total bandwidth of the network. Figure 16 shows that TCP and DCTCP perform significantly worse than others, because they do not have performance isolation between TCP and UDP flows. HCSFQ performs better than AFQ and SP-PIFO, because AFQ and SP-PIFO map different flows to a small number of queues and aggressive UDP traffic overloads the queues shared by multiple TCP and UDP flows, while HCSFQ drops excessive UDP packets before they enter the queues.

Incast. This experiment evaluates HCSFQ in an incase scenario where a receiver requests for a 4.5MB file distributed over N (=30–180) sender nodes. We follow the common practice to use a small RTO_{min} (200μs) for all schemes [37]. As

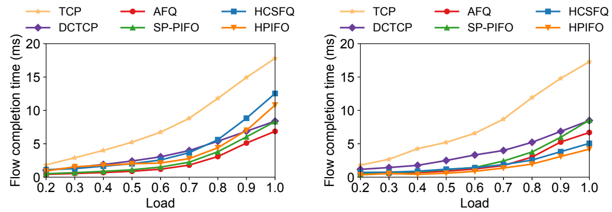

(a) Average flow completion time for flows less than 100KB (Tenant 1).

(b) Average flow completion time for flows less than 100KB (Tenant 2).

Figure 18: Simulation result under the web search workload with two tenants. Tenant 1 sends five times as many flows as tenant 2, and should have higher FCT than tenant 2.

shown in Figure 17(a), when the number of flows grows, HCSFQ achieves a lower request completion time compared with SP-PIFO, TCP and DCTCP, and is close to AFQ. SP-PIFO does not handle the incast traffic pattern well, because there are many packets arriving at the same time with similar ranks saturating some queues and getting dropped. Figure 17(b) shows that HCSFQ achieves low average completion times for individual flows as the number of flows changes.

Web search workload with two tenants. This experiment evaluates hierarchical fair queueing with two tenants. Tenant 1 sends five times as many flows as tenant 2, and the flow size and arriving time follow the web search workload [36]. As shown in Figure 18, HCSFQ can provide tenant-level fairness, so that since tenant 1 has more flows, the average flow completion time of tenant 1 is higher than that of tenant 2. We also implement a hierarchical version of PIFO (HPIFO) as an upper bound for comparison. Note that although HPIFO delivers the best result, it needs to maintain three queues (one in the first layer and two in the second layer) for two tenants. It cannot be implemented on today's switches and it is hard to support many tenants due to the need of hierarchical queues. Other approaches do not distinguish between tenants, and the average flow completion times of the two tenants are similar.

Scalability with many tenants. We show the scalability of HCSFQ on supporting many tenants and flows. When there are many tenants and flows, the share of each tenant/flow is small and the bias from rate estimation and rate update in each step will accumulate. In this experiment, we examine 50 tenants. Half of the tenants (tenant 1-25) have one VM in each server, and the other half (tenant 26-50) have two VMs in each server. Each VM has a long-lasting TCP flow with another VM of the same tenant in another rack. We set the bandwidth of access links and leaf-spine links to 10Gbps and 40Gbps respectively in order to accommodate more tenants and flows than previous experiments. Figure 19 shows that TCP, DCTCP, AFQ and SP-PIFO do not provide tenant-level fairness, and the tenants with more flows have higher total throughput. In comparison, HCSFQ provides fair bandwidth allocation between tenants, regardless of the number of flows each tenant has.

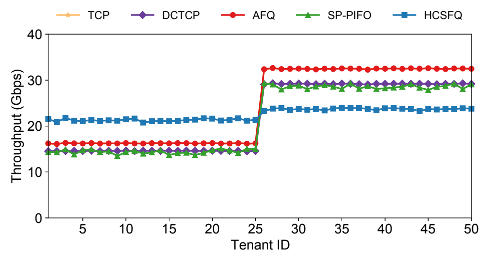

Figure 19: Throughput of different tenants. Each tenant of Tenants 1-25 has one VM in each server, while each tenant of Tenants 26-50 has two VM in each server. Each tenant is sending pairwise TCP traffic between its VMs.

7 Related Work

Fair queueing. There is a long history of work on fair queueing. The original proposal from Nagle [1] introduces the idea of using separate FIFO queues for flows to achieve fair bandwidth allocation. The bit-by-bit round robin (BR) algorithm [2, 3] computes a bid number to estimate the departure time for each packet, and transmits the packet with the lowest bid number with a priority queue. To avoid expensive priority queues, several algorithms, such as SFQ [4] and DRR [5], propose to map flows to a small number of FIFO queues, which do not work well when the number of flows are far larger than the number of queues. Another approach is probabilistic packet dropping, which maintains per-flow state to estimate drop probability, such as FRED [6], RED-PD [7] and AFD [8]. CSFQ [13] is distinct from these algorithms in that it does not require per-flow state, per-flow queues or an expensive priority queue. Hierarchical fair queueing adds a hierarchy to fair queueing, which require not only per-flow state, but also a hierarchy of queues [9, 10, 15]. HCSFQ eliminates both requirements, making hierarchical fair queueing feasible to be implemented in high-speed hardware switches.

Network isolation in multi-tenant cloud. Prior work has proposed techniques to provide performance guarantees and share bandwidth between multiple tenants [14, 16–28, 38, 39]. However, existing works either can only enforce hierarchical fairness at end hosts, or can not be efficiently implemented in today's hardware. For example, BwE [39] is a WAN bandwidth allocation mechanism which enforces hierarchical fair allocation at end hosts. FairCloud [14] proposes to apply CSFQ for network isolation in datacenters, but it does not have a hardware implementation for CSFQ and does not support hierarchical fair queueing. HCSFQ is to the best of our knowledge, the *first* solution to provide hierarchical fair queueing on commodity switches with small switch memory footprint and a single FIFO queue.

Programmable switches. Programmable switches have triggered many innovations in recent years [32, 40–60]. Programmable packet scheduling is the most relevant to HCSFQ. UPS [61] shows that Least Slack Time First (LSTF) provides a good approximation for many scheduling algorithms in practice. PIFO [10] provides a hardware design to realize the abstraction of a push-in first-out (PIFO) queue. It relies on a tree of PIFO queues to implement hierarchical fair queueing. AFQ [11] approximates fair queueing by using a few queues to emulate many queues. It stores per-flow counters in a count-min sketch, and does not support hierarchical fair queueing. SP-PIFO [12] uses several strict priority queues to emulate a PIFO queue, which can support fair queueing, not hierarchical fair queueing. Compared to them, we show how to leverage programmable switches to support fair queueing without per-flow state based on CSFQ, and present a new algorithm HCSFQ to support hierarchical fair queueing.

8 Conclusion

We present HCSFQ, a scalable algorithm for hierarchical fair queueing. Hierarchical fair queueing is a long standing problem in networking. Instead of relying on a hierarchy of queues with complex queue management, HCSFQ only keeps the state for the interior nodes and uses only one queue to achieve hierarchical fair queueing. This dramatically simplifies the design, and makes the design possible to be implemented in high-speed switches. Indeed, we have built a prototype for HCSFQ on programmable switches. Our prototype shows that HCSFQ works well with both UDP and TCP without any changes to either the hardware (e.g., NICs) or software (e.g., TCP/IP stack) of the end hosts.

To the best of our knowledge, HCSFQ is the first solution that has been demonstrated to provide hierarchical fair queueing on hardware switches at line rate. HCSFQ is not only theoretically interesting, but also has important practical implications. Network isolation is critical to multi-tenant clouds, which have a natural two-layer hierarchy. This hierarchy naturally requires the datacenter network to first allocate the bandwidth to the tenants, and then allocate each tenant's bandwidth between the tenant's flows. HCSFQ provides the first solution to enable this two-layer isolation in datacenter networks. Our prototype shows that this can be done without any changes to either the hardware (e.g., NICs) or software (e.g., TCP/IP stack) of the end hosts, and it works well with both UDP and TCP. We believe HCSFQ is a promising solution for network isolation in multi-tenant datacenters.

Acknowledgments

We sincerely thank our shepherd Dongsu Han and the anonymous reviewers for their valuable feedback on earlier versions of this paper. Xin Jin (xinjinpku@pku.edu.cn) is the corresponding author. This work is supported in part by NSF grants CCF-1652257, CNS-1813487 and CCF-1918757, and a Google Faculty Research Award.

References

[1] J. Nagle, "On packet switches with infinite storage," *IEEE Transactions on Communications*, April 1987.

[2] A. Demers, S. Keshav, and S. Shenker, "Analysis and simulation of a fair queueing algorithm," *SIGCOMM CCR*, August 1989.

[3] S. Keshav, "On the efficient implementation of fair queueing," *Internetworking: Research and Experience*, September 1991.

[4] P. E. McKenney, "Stochastic fairness queueing.," in *IEEE INFOCOM*, June 1990.

[5] M. Shreedhar and G. Varghese, "Efficient fair queueing using deficit round robin," in *ACM SIGCOMM*, October 1995.

[6] D. Lin and R. Morris, "Dynamics of random early detection," in *ACM SIGCOMM*, October 1997.

[7] R. Mahajan, S. Floyd, and D. Wetherall, "Controlling high-bandwidth flows at the congested router," in *IEEE ICNP*, November 2001.

[8] R. Pan, L. Breslau, B. Prabhakar, and S. Shenker, "Approximate fairness through differential dropping," *SIGCOMM CCR*, April 2003.

[9] J. C. Bennett and H. Zhang, "Hierarchical packet fair queueing algorithms," in *ACM SIGCOMM*.

[10] A. Sivaraman, S. Subramanian, M. Alizadeh, S. Chole, S.-T. Chuang, A. Agrawal, H. Balakrishnan, T. Edsall, S. Katti, and N. McKeown, "Programmable packet scheduling at line rate," in *ACM SIGCOMM*, August 2016.

[11] N. K. Sharma, M. Liu, K. Atreya, and A. Krishnamurthy, "Approximating fair queueing on reconfigurable switches," in *USENIX NSDI*, April 2018.

[12] A. G. Alcoz, A. Dietmüller, and L. Vanbever, "SP-PIFO: Approximating push-in first-out behaviors using strict-priority queues," in *USENIX NSDI*, February 2020.

[13] I. Stoica, S. Shenker, and H. Zhang, "Core-stateless fair queueing: Achieving approximately fair bandwidth allocations in high speed networks," in *ACM SIGCOMM*, October 1998.

[14] L. Popa, G. Kumar, M. Chowdhury, A. Krishnamurthy, S. Ratnasamy, and I. Stoica, "Faircloud: Sharing the network in cloud computing," in *ACM SIGCOMM*, August 2012.

[15] S. Floyd and V. Jacobson, "Link-sharing and resource management models for packet networks," *IEEE/ACM Transactions on Networking*, August 1995.

[16] H. Ballani, P. Costa, T. Karagiannis, and A. Rowstron, "Towards predictable datacenter networks," in *ACM SIGCOMM*, August 2011.

[17] H. Ballani, K. Jang, T. Karagiannis, C. Kim, D. Gunawardena, and G. O'Shea, "Chatty tenants and the cloud network sharing problem," in *USENIX NSDI*, April 2013.

[18] C. Guo, G. Lu, H. J. Wang, S. Yang, C. Kong, P. Sun, W. Wu, and Y. Zhang, "SecondNet: A data center network virtualization architecture with bandwidth guarantees," in *ACM CoNEXT*, November 2010.

[19] D. Xie, N. Ding, Y. C. Hu, and R. Kompella, "The only constant is change: Incorporating time-varying network reservations in data centers," in *ACM SIGCOMM*, August 2012.

[20] S. Angel, H. Ballani, T. Karagiannis, G. O'Shea, and E. Thereska, "End-to-end performance isolation through virtual datacenters," in *USENIX OSDI*, October 2014.

[21] J. Lee, Y. Turner, M. Lee, L. Popa, S. Banerjee, J.-M. Kang, and P. Sharma, "Application-driven bandwidth guarantees in datacenters," in *ACM SIGCOMM*, August 2014.

[22] H. Rodrigues, J. R. Santos, Y. Turner, P. Soares, and D. O. Guedes, "Gatekeeper: Supporting bandwidth guarantees for multi-tenant datacenter networks.," in *Workshop on I/O Virtualization*, June 2011.

[23] K. Jang, J. Sherry, H. Ballani, and T. Moncaster, "Silo: Predictable message latency in the cloud," in *ACM SIGCOMM*, August 2015.

[24] A. Shieh, S. Kandula, A. G. Greenberg, C. Kim, and B. Saha, "Sharing the data center network," in *USENIX NSDI*.

[25] V. T. Lam, S. Radhakrishnan, R. Pan, A. Vahdat, and G. Varghese, "NetShare and stochastic NetShare: Predictable bandwidth allocation for data centers," *SIGCOMM CCR*, June 2012.

[26] V. Jeyakumar, M. Alizadeh, D. Mazières, B. Prabhakar, C. Kim, and A. Greenberg, "EyeQ: Practical network performance isolation at the edge," in *USENIX NSDI*, April 2013.

[27] L. Popa, P. Yalagandula, S. Banerjee, J. C. Mogul, Y. Turner, and J. R. Santos, "ElasticSwitch: Practical work-conserving bandwidth guarantees for cloud computing," in *ACM SIGCOMM*, August 2013.

[28] M. Chowdhury, Z. Liu, A. Ghodsi, and I. Stoica, "HUG: Multi-resource fairness for correlated and elastic demands," in *USENIX NSDI*, March 2016.

[29] "Barefoot Tofino." https://www.barefootnetworks.com/technology/#tofino.

[30] "Broadcom Ethernet Switches and Switch Fabric Devices."

[31] "Cavium XPliant," 2018. https://www.cavium.com/.

[32] R. Miao, H. Zeng, C. Kim, J. Lee, and M. Yu, "Silkroad: Making stateful layer-4 load balancing fast and cheap using switching ASICs," in *ACM SIGCOMM*, August 2017.

[33] M. Mathis, J. Semke, J. Mahdavi, and T. Ott, "The macroscopic behavior of the TCP congestion avoidance algorithm," *SIGCOMM CCR*, July 1997.

[34] "Intel data plane development kit (dpdk)," 2018. http://dpdk.org/.

[35] "Netbench." http://github.com/ndal-eth/.

[36] M. Alizadeh, S. Yang, M. Sharif, S. Katti, N. McKeown, B. Prabhakar, and S. Shenker, "pfabric: minimal near-optimal datacenter transport," in *ACM SIGCOMM*, 2013.

[37] V. Vasudevan, A. Phanishayee, H. Shah, E. Krevat, D. G. Andersen, G. R. Ganger, G. A. Gibson, and B. Mueller, "Safe and effective fine-grained tcp retransmissions for datacenter communication," *SIGCOMM CCR*, August 2009.

[38] P. Kumar, N. Dukkipati, N. Lewis, Y. Cui, Y. Wang, C. Li, V. Valancius, J. Adriaens, S. Gribble, N. Foster, and A. Vahdat, "PicNIC: Predictable virtualized NIC," in *ACM SIGCOMM*, August 2019.

[39] A. Kumar, S. Jain, U. Naik, A. Raghuraman, N. Kasinadhuni, E. C. Zermeno, C. S. Gunn, J. Ai, B. Carlin, M. Amarandei-Stavila, *et al.*, "Bwe: Flexible, hierarchical bandwidth allocation for wan distributed computing," in *ACM SIGCOMM*, August 2015.

[40] N. K. Sharma, A. Kaufmann, T. E. Anderson, A. Krishnamurthy, J. Nelson, and S. Peter, "Evaluating the power of flexible packet processing for network resource allocation.," in *USENIX NSDI*, March 2017.

[41] K.-F. Hsu, R. Beckett, A. Chen, J. Rexford, P. Tammana, and D. Walker, "Contra: A programmable system for performance-aware routing," in *USENIX NSDI*, February 2020.

[42] "In-band Network Telemetry (INT) Dataplane Specification." https://github.com/p4lang/p4-applications/blob/master/docs/INT.pdf.

[43] A. Gupta, R. Harrison, M. Canini, N. Feamster, J. Rexford, and W. Willinger, "Sonata: Query-driven streaming network telemetry," in *ACM SIGCOMM*, August 2018.

[44] S. Narayana, A. Sivaraman, V. Nathan, P. Goyal, V. Arun, M. Alizadeh, V. Jeyakumar, and C. Kim, "Language-directed hardware design for network performance monitoring," in *ACM SIGCOMM*, August 2017.

[45] N. Katta, M. Hira, C. Kim, A. Sivaraman, and J. Rexford, "Hula: Scalable load balancing using programmable data planes," in *ACM SOSR*, March 2016.

[46] X. Jin, X. Li, H. Zhang, R. Soulé, J. Lee, N. Foster, C. Kim, and I. Stoica, "NetCache: Balancing key-value stores with fast in-network caching," in *ACM SOSP*, October 2017.

[47] Z. Liu, Z. Bai, Z. Liu, X. Li, C. Kim, V. Braverman, X. Jin, and I. Stoica, "DistCache: Provable load balancing for large-scale storage systems with distributed caching," in *USENIX FAST*, February 2019.

[48] M. Liu, L. Luo, J. Nelson, L. Ceze, A. Krishnamurthy, and K. Atreya, "IncBricks: Toward in-network computation with an in-network cache," in *ACM ASPLOS*, April 2017.

[49] X. Jin, X. Li, H. Zhang, N. Foster, J. Lee, R. Soulé, C. Kim, and I. Stoica, "NetChain: Scale-free sub-RTT coordination," in *USENIX NSDI*, April 2018.

[50] H. T. Dang, D. Sciascia, M. Canini, F. Pedone, and R. Soulé, "NetPaxos: Consensus at network speed," in *ACM SOSR*, June 2015.

[51] H. T. Dang, M. Canini, F. Pedone, and R. Soulé, "Paxos made switch-y," *SIGCOMM CCR*, April 2016.

[52] D. R. K. Ports, J. Li, V. Liu, N. K. Sharma, and A. Krishnamurthy, "Designing distributed systems using approximate synchrony in data center networks," in *USENIX NSDI*, May 2015.

[53] J. Li, E. Michael, N. K. Sharma, A. Szekeres, and D. R. Ports, "Just say NO to Paxos overhead: Replacing consensus with network ordering," in *USENIX OSDI*, November 2016.

[54] H. Zhu, Z. Bai, J. Li, E. Michael, D. Ports, I. Stoica, and X. Jin, "Harmonia: Near-linear scalability for replicated storage with in-network conflict detection," in *Proceedings of the VLDB Endowment*, November 2019.

[55] J. Li, E. Michael, and D. R. K. Ports, “Eris: Coordination-free consistent transactions using in-network concurrency control,” in *ACM SOSP*, October 2017.

[56] A. Lerner, R. Hussein, P. Cudre-Mauroux, and U. eXascale Infolab, “The case for network accelerated query processing.,” in *CIDR*, January 2019.

[57] A. Sapio, I. Abdelaziz, A. Aldilaijan, M. Canini, and P. Kalnis, “In-network computation is a dumb idea whose time has come,” in *ACM SIGCOMM HotNets Workshop*, November 2017.

[58] A. Sapio, M. Canini, C.-Y. Ho, J. Nelson, P. Kalnis, C. Kim, A. Krishnamurthy, M. Moshref, D. R. Ports, and P. Richtárik, “Scaling distributed machine learning with in-network aggregation,” *arXiv preprint arXiv:1903.06701*, February 2019.

[59] N. Ivkin, Z. Yu, V. Braverman, and X. Jin, “Qpipe: Quantiles sketch fully in the data plane,” in *ACM CoNEXT*, December 2019.

[60] Z. Yu, Y. Zhang, V. Braverman, M. Chowdhury, and X. Jin, “Netlock: Fast, centralized lock management using programmable switches,” in *ACM SIGCOMM*, August 2020.

[61] R. Mittal, R. Agarwal, S. Ratnasamy, and S. Shenker, “Universal packet scheduling,” in *USENIX NSDI*, March 2016.

A Proof of Theorem 1

Proof. The first conclusion is directly derived from the guarantee of CSFQ [13].

For the second conclusion, we consider a model with a parent and k children. We add a script $'$ to represent the notations related to the parent, e.g., r'_i is the estimated arrival rate of the i-th packets at the parent. We add a script (j) to represent the notations related to the j-th child, e.g., $r_i^{(j)}$ is the estimated arrival rate of the i-th packets at the j-th child. Suppose the time episode is universal for all children. Suppose that $r_0^{(j)} = r'_0 = 0$ for $j = 1, \ldots, k$.

Suppose the inter-arrival time $T_i \geq \tau$ for all i. Suppose

$$r_{\alpha'} \geq \frac{1}{1-e^{-\tau/K}} \sum_{j=1}^{k} r_\alpha^{(j)}.$$

Then we will show that the parent node $r_{\alpha'}$ does not drop packets. To this end, we only need to prove that

$$r'_i \leq r_{\alpha'}, \quad \forall i. \tag{9}$$

After the first drop, the package length is $h_i = h_i^{(1)} + \cdots + h_i^{(k)}$, where

$$h_i^{(j)} = \begin{cases} \ell_i^{(j)} & r_i^{(j)} \leq r_\alpha^{(j)}, \\ \ell_i^{(j)} \frac{r_\alpha^{(j)}}{r_i^{(j)}} & r_i^{(j)} > r_\alpha^{(j)}. \end{cases}$$

And by definition,

$$r'_i = (1-e^{-T_i/K})\frac{h_i}{T_i} + e^{-T_i/K} r'_{i-1}, \quad 1 \leq i \leq n.$$

We now recursively prove Eq. (9).

(i) First let $i = 1$.

We will use the following inequality to prove Eq. (9):

$$(1-e^{-T_1/K})\frac{h_1^{(j)}}{T_1} \leq r_\alpha^{(j)}, \quad \forall j. \tag{10}$$

On the one hand, if Eq. (10) is true, we have

$$r'_1 = (1-e^{-T_1/K})\frac{\sum_{j=1}^{k} h_1^j}{T_1} \leq \sum_{j=1}^{k} r_\alpha^j \leq r_{\alpha'},$$

which implies Eq. (9) for $i = 1$.

On the other hand, recall $r_1^{(j)} = (1-e^{-T_1/K})\frac{\ell_1^{(j)}}{T_1}$, we then prove Eq. (10) as following:

1. If $r_1^{(j)} < r_\alpha^{(j)}$, then $h_1^{(j)} = \ell_1^{(j)}$, thus

$$(1-e^{-T_1/K})\frac{h_1^{(j)}}{T} = (1-e^{-T_1/K})\frac{\ell_1^{(j)}}{T} = r_1^{(j)} \leq r_\alpha^{(j)}.$$

2. If $r_1^{(j)} \geq r_\alpha$, then $h_1^{(j)} = \ell_1^{(j)} \frac{r_\alpha^{(j)}}{r_1^{(j)}}$, thus

$$(1-e^{-T_1/K})\frac{h_1^{(j)}}{T_1} = (1-e^{-T_1/K})\frac{\ell_1^{(j)}}{T_1}\frac{r_\alpha^{(j)}}{r_1^{(j)}} = r_\alpha^{(j)}.$$

Thus Eq. (10) holds.

(ii) Now suppose that $r'_{i-1} \leq r_{\alpha'}$.

We will use the following inequality to prove our claim:

$$(1-e^{-T_i/K})\frac{h_i^{(j)}}{T_i} \leq r_\alpha^{(j)}, \quad \forall j. \tag{11}$$

On the one hand, if Eq. (11) is true, we have

$$\begin{aligned} r'_i =& (1-e^{-T_i/K})\frac{\sum_{j=1}^{k} h_i^{(j)}}{T_i} + e^{-T_i/K} r'_{i-1} \\ \leq& \sum_{i=1}^{k} r_\alpha + e^{-a/K} r'_\alpha \leq r'_\alpha, \end{aligned}$$

which implies Eq. (9) for i.

On the other hand, recall

$$r_i^{(j)} = (1-e^{-T_i/K})\frac{\ell_i^{(j)}}{T_i} + e^{-T_i/K} r_{i-1}^{(j)},$$

we then prove Eq. (11) as following:

1. If $r_i^{(j)} < r_\alpha^{(j)}$, then $h_i^{(j)} = \ell_i^{(j)}$, thus

$$\begin{aligned} (1-e^{-T_i/K})\frac{h_i^{(j)}}{T_i} =& (1-e^{-T_i/K})\frac{\ell_i^{(j)}}{T_i} \\ =& r_i^{(j)} - e^{-T_i/K} r_{i-1}^{(j)} \\ \leq& r_i^{(j)} \leq r_\alpha^{(j)}. \end{aligned}$$

2. If $r_i^{(j)} \geq r_\alpha^{(j)}$, then $h_i^{(j)} = \ell_i^{(j)} \frac{r_\alpha^{(j)}}{r_i}^{(j)}$, thus

$$\begin{aligned} (1-e^{-T_i/K})\frac{h_i^{(j)}}{T_i} =& (1-e^{-T_i/K})\frac{\ell_i^{(j)}}{T_i}\frac{r_\alpha^{(j)}}{r_i^{(j)}} \\ =& (r_i^{(j)} - e^{-T_i/K} r_{i-1}^{(j)})\frac{r_\alpha^{(j)}}{r_i^{(j)}} \\ \leq& r_i^{(j)} \frac{r_\alpha^{(j)}}{r_i^{(j)}} = r_\alpha^{(j)}. \end{aligned}$$

Thus Eq. (10) holds. By (i) and (ii) and mathematical induction our proof is finished. □